CERN-SPSC/89-55
SPSC/P238Add.2
14 September, 1989

Addendum to Proposal P238:

REQUEST FOR COLLIDER TEST OF SILICON MICROVERTEX DETECTOR

A. Brandt, S. Erhan, D. Lynn, M. Medinnis, P. Schlein*, J. Zweizig
University of California, Los Angeles, U.S.A.

P. Weilhammer[1]
CERN, Geneva, Switzerland

T. Ypsilantis
College de France[2], Paris, France

G. Borreani
University of Ferrara and INFN[3], Italy

A. Kaschuk, V. Samsonov, V. Sarantzev, E. Spiridenkov, A. Vorobyov
Institute for Nuclear Physics, Gatchina, Leningrad, U.S.S.R.

M. Calvetti
University of Perugia and INFN[3], Italy

J.B. Cheze, J. Zsembery
Centre d'Etudes Nucleaires – Saclay[4], Gif-sur-Yvette, France

R. Dzhelyadin, Y. Guz, V. Kubic, V. Obraztsov, A. Ostankov
IHEP-Serpukhov, Protvino, U.S.S.R.

C. Biino, R. Cester, A. Migliori, R. Mussa, S. Palestini
University of Torino and INFN[3], Italy

ABSTRACT

We request a collider run during the fall of 1990, in order to test the silicon micro-vertex detector proposed in P238. To be certain that the proposed trigger will function correctly, we should verify that real data, taken in situ under the same conditions of the experiment (including present low-β machine configuration), are in essential agreement with the Monte Carlo simulation data used in the trigger design of P238. Revised (conservative) event yield estimates and a first analysis of simulated RICH counter data for B_s are also given.

---

*) Spokesman
[1]) At this time, commitment is for silicon test run
[2]) Pending approval of the Laboratory and IN2P3
[3]) Pending approval of INFN
[4]) Pending approval of CEN-Saclay

TABLE OF CONTENTS

APPENDICES

1. Introduction

In the documents, P238 and P238Add.1, we have proposed a new approach to the study of B (beauty or bottom) physics at hadron colliders. Forward detectors installed on the outgoing arms of an interaction region provide adequate acceptance of the forward-collimated decay products of B-mesons. The reconstruction of exclusive final states in B-decay with minimal background is made possible with the use of a silicon microvertex detector, whose elements are installed perpendicular to the beam, inside the vacuum pipe and dispersed throughout ± 30 cm of the interaction region. Data acquisition is triggered by the results of high speed digital calculations based on the silicon data and performed with the use of a data-driven processor.

The efficient triggering of heavy flavor in hadron machines was long thought to be "next to impossible". However, the success of Fermilab Experiment E691 and its successor in obtaining large clean samples of charmed particles has partly dispelled this "myth". Now, with the several physicist-years of Monte Carlo simulation work reported in P238, we have demonstrated that it should be possible to advance one step further by triggering on and obtaining, at the much higher energy hadron colliders, relatively clean and large samples of beauty mesons.

While there are many challenging hardware components in the proposed Forward Beauty Detector (FBD), only the operation of the silicon detectors within the SPS vacuum chamber has intrinsic uncertainties which could influence the overall success of the experiment. These major uncertainties are the amounts of event-unrelated noise and beam halo tracks which will be recorded by the silicon detectors. Since we have shown, in Appendix A of P238, that the PYTHIA-generated minimum bias events are in good agreement with the minimum bias data from Experiment UA5, it is likely that only such (unanticipated) event-unrelated "noise" in the silicon could, a priori, present serious difficulties.

In order to determine the magnitude of such contributions to the observed silicon signals, and thus the reliability of the proposed trigger in the complete experiment, it is essential to have a preliminary run at the collider with elements of the silicon microvertex detector installed in the manner proposed in P238, and with the same low-β machine configuration that will be required by the full experiment (straight section ± 13 meters). If the silicon data thus obtained is similar to our Monte Carlo simulated silicon data, the proposed trigger will work as required.

2. Goals of Collider Test Run

The collider test will be carried out with the following goals in mind:

- Write events on tape, using a minimum bias trigger (beam crossing signal in coincidence with signals from a modest scintillator hodoscope), to verify and tune (offline) both our Monte Carlo simulation and the trigger described in proposal P238. This will also allow an evaluation of the effects of background sources such as beam halo, which are not included in the simulation. With this data we will be able to improve the present trigger algorithm and evaluate (and invent) other, possibly more effective, trigger algorithms.

- It should be possible to clearly demonstrate evidence for events which contain B hadrons by track reconstruction (straight lines) in events with multiple high multiplicity secondary vertices. We estimate that 10^7 events on tape will yield approximately 100 events with visible B hadrons. Detailed estimates are being made of the fraction of these which will be distinguishable from the more abundant charmed particle events.

- Measure radiation doses to detector and readout electronics. For a number of reasons, we are reasonably confident that radiation is not a problem: (a) our silicon detectors will be retracted about 10 cm from the beam line when the machine is not in "stable beam" state; (b) from measurements made by UA8, the halo rate under normal operating conditions is rather small;

(c) the beam-beam interaction rate is not high enough to cause difficulties. We will nonetheless take this opportunity to install dosimeters at various places within the detector volume.

- Test the precision and reproducibility of the detector positioning mechanism using reconstructed tracks in the silicon. Although such tests could be done in a fixed target test beam, the completed silicon mechanics system (see Section 4 below) is not likely to be available before the end of the fixed target run in June, 1990.

Finally, we note that, in Appendix A of P238Add.1, we described the current status of the data-driven processor. Development of the software package which will allow emulation of the full trigger processor is in progress with very high priority and production (replication) of the hardware modules should be completed early in 1990. Although the online use of the processor does not constitute an uncertainty in the same class as those mentioned above, it will nonetheless be possible to have a smaller version of the full processor running on-line by the time of the collider run (about 30 modules out of the full set of about 260 modules). This test processor configuration would include one of the eight 3-point line-finding subroutines of the final processor configuration, a duplicate rejection subroutine and a first vertex estimator and would be capable of online reconstruction of the tracks and calculation of the vertex position (using the first-vertex estimate described in Section 4.3 of P238).

3. Silicon Detectors

The following two paragraphs are from Appendix B of P238Add.1.

> In our simulation work (including that presented in this addendum), we assume a vertex detector consisting of 11 parallel planes, spaced 6 cm apart, with each plane divided into four 7 × 7 cm^2 silicon squares (see section 4.1 of the P238 proposal). The silicon planes are assumed to be 200 μm thick and to have 25 μm strips on both sides.
>
> After discussions with manufacturers, we have come to realize that such a scheme is not feasible, primarily because the 7 × 7 cm^2 size is too large to comfortably fit on the standard 4 inch diameter silicon wafers. We have thus revised our detector design. We are now considering a detector which consists of sixteen parallel 10 × 10 cm^2 detector planes divided into four 5 × 5 cm^2 squares, spaced 4 cm apart. The detector is otherwise the same as that presented in the proposal.

In order to keep the detector for the test run as simple as possible, consistent with attaining the goals listed in Section 2, a subset of the full 16-plane detector system will be used. Fig. 1 shows the 6-plane system which will be constructed. The planes are perpendicular to the beam line and are spaced every 4 cm. Each detector consists of independent upper and lower assemblies, each of which comprises two 5 cm x 5 cm detectors side by side. The detectors will only have vertical microstrips. We can thus save considerable money and effort while still meeting the goals of the proposed test.

With the 6-plane geometry of the test detector, about one third of all events will occur in a roughly 8 cm long region, which will allow reconstruction of tracks with at least three hits in one hemisphere and tracks with two hits in the opposite hemisphere.

Since the version of the Berkeley SVX chip intended for use in the final experiment will not be available until 1991, we will use the current SVX chip (Version D). This chip is a production version and is now being installed on the CDF microvertex detector. For the test run, we will read out the charge associated with all hit strips.

Because Version D of the SVX chip is designed to couple to 50 μ pitch silicon detectors, the detectors used in the test run will have 50 micron pitch instead of the 25 micron pitch of the detectors in the final experiment. Since the configuration to be used in the test will only measure coordinates in the horizontal view, there will be a total of about 24,000 channels.

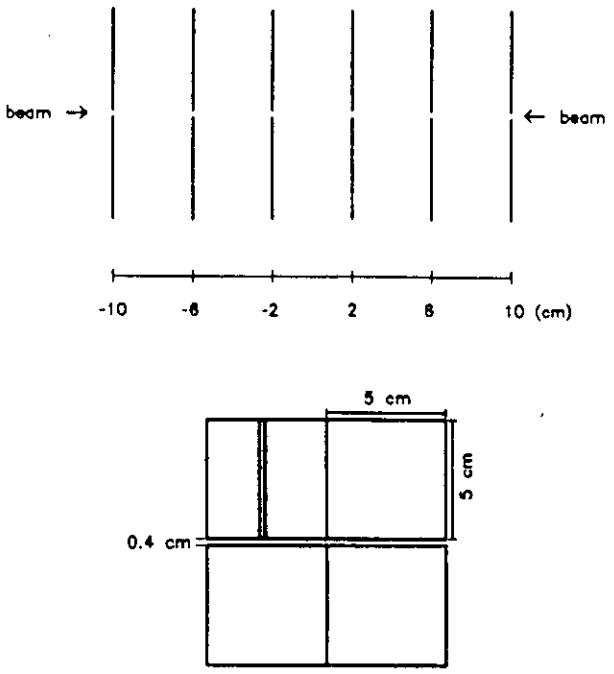

Figure 1: Proposed 6-plane silicon detector system for collider test run. Side view shows the 4 cm spacing between planes. and the independent upper and lower detector assemblies. The beams pass through the 4 mm gap between these assemblies. The front view shows how the upper and lower assemblies each contain two 5 cm x 5 cm silicon detectors side by side.

4. Support Mechanics & RF Shielding

The essential requirements for the silicon support mechanics are discussed on pages 16-18 of P238. These have been discussed with members of the SPS vacuum group and various ideas on how to achieve them have evolved. In particular, Hartmuth Wahl of that group has suggested a scheme, whereby the silicon detectors are isolated from the main machine vacuum by a window which would also provide sufficient shielding against RF pickup by the silicon detectors due to the passing beam bunches.

It has been suggested to us that the Vacuum Group might be able to assist us in some preliminary tests of the RF pickup problem by constructing a model chamber in which one of our presently running silicon detectors is positioned close to a long wire, through which a current pulse is passed to simulate the passage of a beam bunch. Such a test would give us a first estimate of the amount of shielding necessary in the construction of the full mechanical system.

It is our understanding that Hartmuth Wahl has communicated to Pierre Darriulat his assessment that the complete silicon mechanics system could be designed and constructed to be ready for a fall 1990 run in the collider. From our side, we would have the necessary detectors tested and ready for installation on the mechanics system several months before the run.

5. Preparation Timetable for Collider Test Run

Due to the effort made in preparing silicon detectors for a test run in one of the UA8 Roman pot spectrometers during the 1989 run of the SPS-Collider, we already have all necessary SVX-chip readout electronics and relevant software fully operational and interfaced to an online MicroVax computer. We plan to install this equipment as a silicon test setup in a fixed target test beam during the next few weeks. With this test setup, we will test and compare silicon detectors from three sources, The Central Institute for Industrial Research[1] (Oslo), Hamamatsu and Micron.

We already have Hamamatsu and Micron detectors with SVX readout chips bonded to them. They are thus ready to be installed in a test beam. We can bond an existing SVX chip to one of the Oslo detectors in a short time and thus be ready to compare the readout of all three detector types with that chip.

We should have all tests completed by the end of this year, in time to have completed production runs of the necessary detectors and SVX chips on the necessary time scale. We will be ready for the mechanical interface of the detectors with the mechanical support structures provided by the SPS Division, in time for a fall 1990 Collider run.

6. Timetable for Complete Experiment

If design work of the other detector components (magnets, chambers, lead-glass calorimeter and RICH detectors) is carried out in parallel with preparations for this proposed silicon test, it should be possible to go into full production before the end of 1990. With some considerable effort (and help from CERN), it may be possible to have a completed detector ready for use before the end of 1992.

---

[1] The Oslo source manufactures capacitively-coupled strip detectors with integrated polysilicon bias resistors, which were pioneered by P. Weilhammer and T.E. Hansen [see: M. Cacccia et al., NIM A260 (87)124]. The advantage of this approach over other detectors now in use is the elimination of d.c. offsets which can be caused by channel-dependent leakage currents. Such detectors have been developed for use in the DELPHI microvertex detector and are found to give reproducible results within very tight specifications. The possibility of also conveniently reading out the n-side (back-side readout) is a very promising aspect which could be very useful for us in the construction of the final complete silicon trigger detector.

APPENDIX A: REVIEW OF EVENT YIELD ESTIMATES IN P238Add.1

We have reviewed our estimates of B_s and $\bar{B}_s$ event yields in P238Add.1 and adjusted several of the assumed efficiencies and branching ratios in an attempt to provide a more conservative view of the situation. Table 1 is a revised version of Table 2 in P238Add.1 and contains the new estimates. With two arms instrumented and Lead-Glass electromagnetic calorimetry, 1900 reconstructed B_s-mesons should result per 10 pbarn^{-1} integrated luminosity (with Liquid-Xenon calorimetry, 2800 events result). Thus, with one arm instrumented and Lead-Glass calorimetry, approximately 1000 events could be obtained per 10 pbarn^{-1}. This should be sufficient for an excellent measurement of $\Delta M/\Gamma$, although the additional factor of two statistics available with a second instrumented arm would be comforting.

Table 1: Revised B_s & $\bar{B}_s$ Event Yields

$1.5 \cdot 10^8$ $b\bar{b}$ Produced for $\int \mathcal{L} dt = 10$ pbarn^{-1}

1.8×10^7 B_s	1.8×10^7 $\bar{B}_s$	0.12 = B_s Production
5.4×10^6	5.4×10^6	0.30 = 2-Arm Geometrical Acceptance
4.9×10^5	4.9×10^5	0.09 = BR($B_s \rightarrow D_s^*$, D_s and DK with nπ
4.9×10^5	4.9×10^5	1.00 = BR($D_s^* \rightarrow D_s \gamma$)
2.4×10^4	2.4×10^4	0.05 = BR($D_s \rightarrow KK\pi$, $KK3\pi$, K^0K)
1.7×10^4	1.7×10^4	0.68 = No Other Interaction in Bunch Crossing
1.6×10^4	1.6×10^4	0.94 = Vertex Acceptance of Silicon μVertex
6.5×10^3	6.5×10^3	0.42 = Trigger Efficiency (D_s^* 3π)
3.3×10^3	3.3×10^3	0.50 = Event Efficiency Due to Track Finding Losses
1400 B_s	1400 $\bar{B}_s$	0.43 = Event Reconstruction Assumes Liquid-Xenon e.m. calorimetry.
950 B_s	950 $\bar{B}_s$	0.29 = Event Reconstruction Assumes Lead-Glass e.m. calorimetry.

The five parameters that have been changed are discussed in the following paragraphs.

- We now take the $b\bar{b}$ total cross section to be 15 μbarn. The 10 μbarn value previously used corresponded to a $|y| < 1.5$ rapidity cut [K. Ellis, private communication]. This yields a $b\bar{b}$ production sample of 1.5×10^8 events per 10 pbarn^{-1}.

- We now assume that a $\bar{b}$-quark has a 12% probability to combine with an s-quark to make a B_s-meson. This should allow, for example, for the loss of excited B_s which can decay into $D + K$ [V. Khoze, private communication].

- B_s Branching Ratios – We assume BR = 9% for the total of all reactions of the type:

$$B_s \rightarrow D_s^* + n\pi^{\pm}\,,\; D_s + n\pi\,,\; D_u + Kn\pi$$

  We noted in Table 7, page 56 of P238 that the observed ARGUS BR = 6.7% for reactions of the type $B_d \rightarrow D^* + n\pi$ with n = 1,2,3 [H. Schroeder, Rapporteur Talk at XXIV International Conference in HEP (August 1988 - Munich, FRG) and DESY 88-101]. We also assume that the D_s^* to direct D_s ratio is 3/1 and that the final state $D_u Kn\pi$ contributes at least 0.2 %, giving us the total of 9%. Since it seems likely that we shall also be able to reconstruct such final states with n > 3, our effective useful BR should be larger than this.

- $D_s^{\pm}$ Branching Ratio – We now take BR = 5% for all known charged final states: $K^+K^-\pi^{\pm}$, $K^+K^-3\pi$, $K^0K^{\pm}$ [P. Karchin, Rapporteur Talk at SLAC Lepton-Photon Conference (August 1989)].

- Event Efficiency Due to Track Finding Losses – We now assume a total event finding efficiency of 50% due to all possible track losses. This should be a very conservative assumption.

APPENDIX B: MONTE CARLO SIMULATION AND ANALYSIS OF RICH COUNTER DATA

In all our simulation and reconstruction work reported in P238 and P238Add.1, we have assumed that the RICH counter system perfectly identifies all particles. We are now attempting to make a more realistic estimate of the RICH identification efficiencies by simulating the RICH counter response to the tracks from B_s decay and to all other tracks in the detectors. These simulated RICH data are then analyzed, in order to extract identification information for the particles.

In order to obtain an overall efficiency for the RICH identification procedure, we have generated 200 B_s events, in which all particles in the final state $K^+K^-\gamma 4\pi$ (see Eq. 10 in P238Add.1) are contained in the spectrometer aperture. Fig. 2(a) shows the momentum distribution for kaons which emerge from the decay of the B_s. Fig. 2(b) shows the momentum for kaons in the spectrometer which are not from the B_s decay (they provide the K_p and K_s tagging sample discussed in Section 4.2 of P238Add.1). Fig. 3 shows the momentum ranges of unique separation for the indicated particles in the liquid and gas RICH counters.

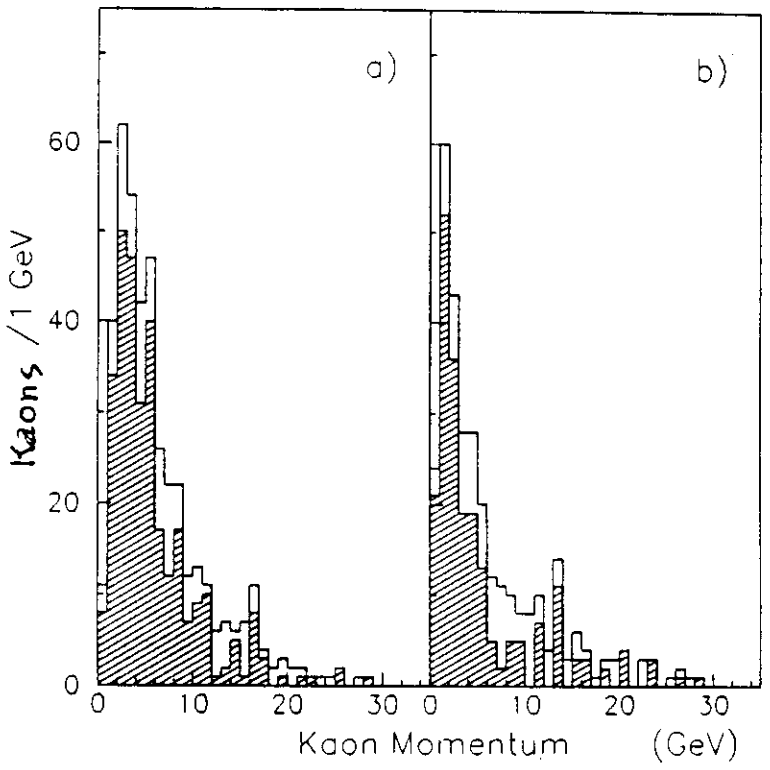

Figure 2: (a) Momentum distribution of $K^{\pm}$ which emerge from $B_s \rightarrow D_s^* 3\pi$ decay. Shaded histogram shows those that enter the first spectrometer (100-600 mrad); (b) Momentum distribution of $K^{\pm}$ in the detector, which do not come from the decay of B_s. Shaded histogram is same as in (a).

We have started by doing an accurate simulation of the Liquid RICH counter in the first (100-600 mrad) spectrometer. The Liquid RICH counters are the most difficult for the following reasons:

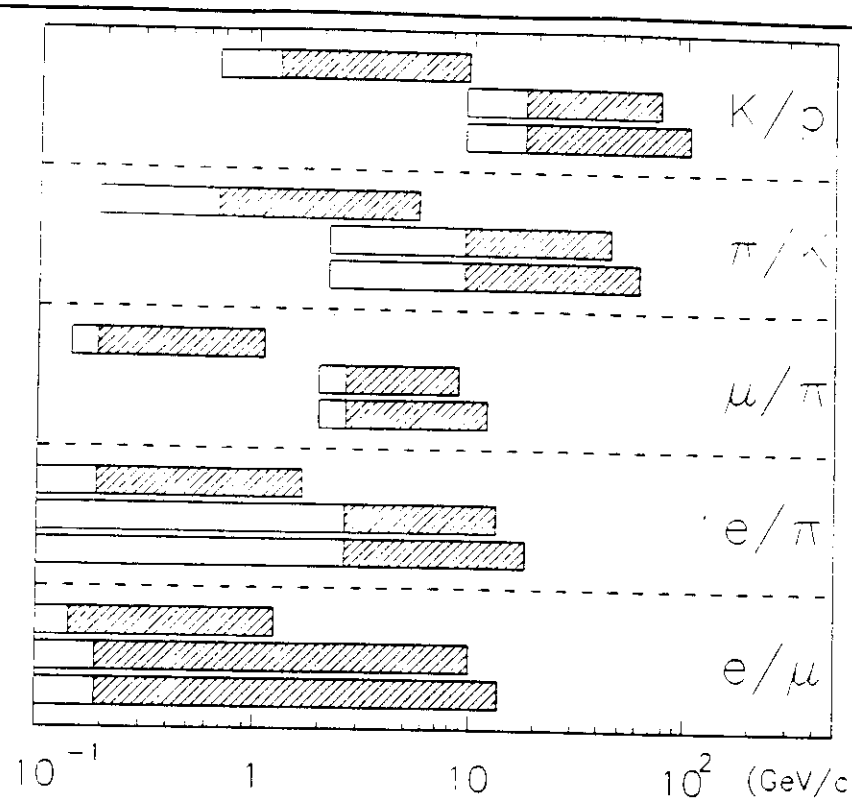

Figure 3: Momentum Ranges of RICH counter Identification. For each indicated pair of particles, the bars at lower momentum are for the liquid RICH counters; the two bars at higher momenta are for the gas RICH counters in the first and second spectrometers, respectively. In all cases, the open bars show the momentum range between the thresholds for the lighter and heavier particles. The upper limits for the hatched bars in all cases show the upper limit for 3σ separation (it is higher for the gas counter of spectrometer 2 because its gas radiator is somewhat longer).

- The number of particles which produce Cerenkov light in the liquid RICH is larger than in the gas counters (pion threshold is about 0.2 GeV/c in the liquid and is about 2.6 GeV/c in the gas counters).

- The "rings" are only rings for particles at normal incidence. Away from normal incidence, the light is seen in conic sections which have been truncated by light loss due to total internal reflection in the liquid radiator.

- The radii of the liquid RICH "rings" are large. Thus, there is considerable overlap of the rings from different particles. There is also some light loss to the walls of the counter.

To illustrate the enormous difference between the signals in the detector planes of both types of counters, we show in Figs. 4(a,b) the detector planes for typical events in, respectively, the liquid and gas RICH counters. For the gas counter, the signals from nine events are superimposed. Note also that the noise signals referred to below are not shown in these figures.

Because the rings in the gas RICH are much much smaller and relatively well isolated, for the purposes of this study, we provisionally assume that the Gas RICH counter perfectly identifies all par-

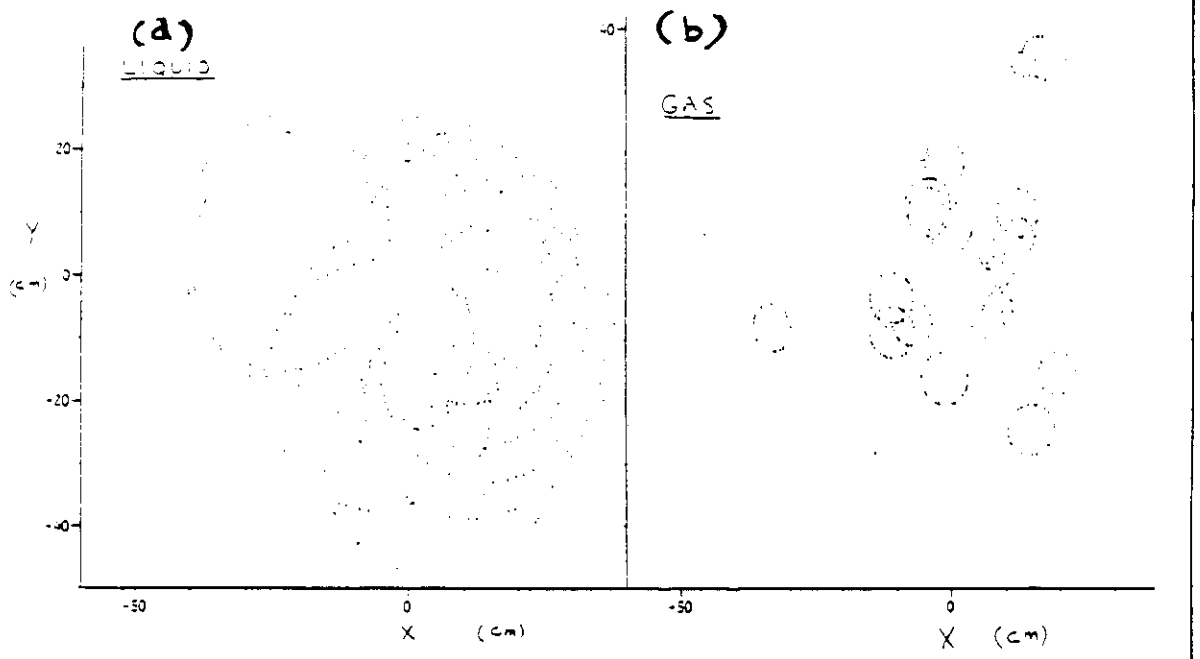

Figure 4: (a) Photon Images for One Typical Event in Detector Plane of Liquid RICH; (b) Photon Images in Detector Plane of Gas RICH. The signals from 9 events are superimposed in the gas RICH figure. Noise signals referred to in the text are not shown in either figure.

ticles for which at least 4 photons are detected. We are in the process of extending our modeling to the entire system and should soon have a more complete answer. We first describe the RICH counter simulation, then the reconstruction algorithm and finally present the results of this study.

RICH Data Simulation

Apart from an approximation described in the next paragraph, the Liquid RICH counter geometry used for this simulation is identical to that described in P238. As shown in Figs. 22 and 38 of P238, the counter consists of a 1 cm thick radiator which is followed by a 3mm thick quartz window. Cerenkov photons which are emitted in the radiator pass through the window into a 25 cm long, helium-filled volume. After traversing the helium, the photons pass through a second quartz window into a photon detector. As described in Section 5.5 of the proposal, this detector consists of a TMAE conversion layer followed by two parallel-plate amplification regions, and a detector with 3×3 mm^2 pixels.

For ease of simulation, all windows, detectors and radiators were assumed to have surfaces perpendicular and parallel to the beam axis. This differs slightly from the proposed geometry in which the normals to the windows are along the average particle direction (see Fig. 22 of P238). This approximation slightly decreases the number of photons detected in a ring image (because of increased losses due to total internal reflection), but should have little effect on the the ring reconstruction problem. In fact, the average number of "detected" photons generated by the program (20) is very close to the 23.4 photons measured by R. Arnold et al. [CRN/HE 87−08] for a $\beta = 1$ track normally incident on a similar prototype module.

All physical effects relating to the generation and propagation of the Cerenkov photons were carefully simulated. Tracks entering the RICH radiator are multiple-scattered between emission of photons. The photons are propagated through the radiator, the two quartz windows and the helium space, taking into account the energy-dependent index of refraction and absorption lengths in each medium. Reflection probabilities are calculated at each interface between two materials with differing indices of refraction and photons were eliminated if reflection takes place. The distance each photon travels in the detector before absorption is then calculated, and the detected photon position is digitized, assuming 3 × 3 mm^2 pads.

Cerenkov light is also generated by all tracks as they traverse the quartz windows (this effect is expected to account for the major fraction of noise photons). These photons are propagated through the counter to the detector in the same manner as those generated in the radiator. It may be noted that the counter configuration used in the present simulation (perpendicular to the beam axis, rather than rotated as in Fig. 22 of P238) overestimates the number of photons from this source, since most photons from tracks normally incident on the quartz are internally reflected in the windows.

Analysis of Simulated RICH Data

The input to our provisional reconstruction algorithm is the list of tracks and their trajectories and momenta, as well as the list of hit RICH detector pads produced by the simulation program. As described below, we assume that, if a particle's velocity is above Cerenkov threshold for pions in the gas RICH counter, the gas counter gives a correct particle identification.

For a given measured charged track, the analysis is based on the reconstruction of a Cerenkov emission angle, θ_c, for each detected photon (at present, each struck 3 x 3 mm^2 pad is interpreted as one photon). A straightforward ray calculation, which includes refraction at the interfaces, gives two equations for the coordinates (x,y) of converted photons in the photon detector as a function of θ_c and the azimuthal Cerenkov emission angle, ϕ_c. For each track, we use these equations and standard numerical techniques to give θ_c and ϕ_c for each detected photon (if a solution exists).

The subsequent analysis is facilitated by the removal of hits in the Liquid RICH detector, which constitute background from two sources:

- For the relatively few tracks in each event which are above Cerenkov threshold in the Gas RICH, a random number, n, is generated according to a Poisson distribution, whose mean is the expected β-dependent photo-electron yield (20 for $\beta = 1$). If $n > 4$, we assume that the Gas RICH counter correctly identifies this track (tracks whose momenta are between pion and kaon thresholds in that counter, and which have no light, are assumed to be kaons). We then remove, from the Liquid RICH hit list, all photons from these tracks which are within 2 standard deviations of their expected θ_c (this standard deviation is discussed in Section 5.5 of P238).

- Cerenkov photons produced in the quartz detector window are removed by removing all hits produced in a 1 cm radius circle about the point where the particle enters the photon detector.

Since, as discussed above, the gas RICH counter is assumed to correctly identify all tracks which are above about 2.6 GeV (pion threshold in that counter), we now investigate with our detailed simulation how well the liquid RICH counter can be used to identify tracks with momentum below 2.6 GeV. Fig. 5 shows a histogram of the values of θ_c for an identified kaon track in a typical B_s event after the above cleanup procedure.. A peak is seen at an angle which corresponds to the Cerenkov emission angle for the track in question. In general, the situation may not be so obvious.

In order to quantify the RICH identification picture, we have employed the following algorithm (somewhat arbitrarily). For each track with momentum below 2.6 GeV, and for each possible mass identity, we count the number of the photons within a "road" of width, $2\sigma_c$, where σ_c is the expected standard deviation on θ_c referred to above (see Section 5.5 of P238). A photon count thus results for

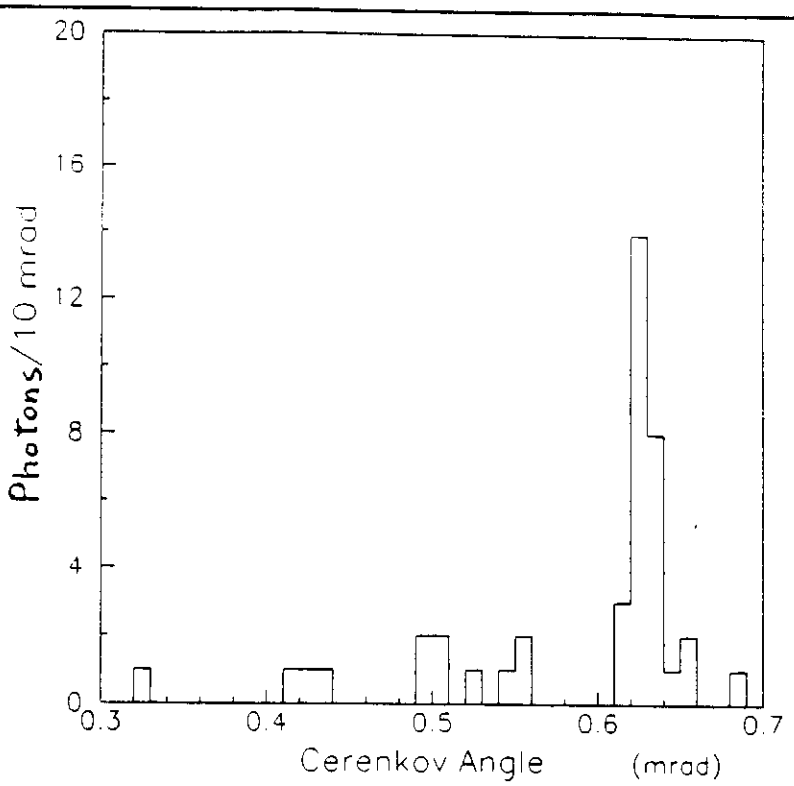

Figure 5: Histogram of reconstructed Cerenkov emission angles for a typical kaon track that is identified by the liquid RICH counter. The momentum of this kaon is 1.7 GeV/c.

each mass identity possibility. For the particle to be uniquely identified as a particular type, the algorithm requires:

- The photon count, $n_\gamma > 5$, within the "road" for that particle type.
- For all other particle types, their photon counts, $n_\gamma' < n_\gamma - 4$.

We are also exploring other more sophisticated algorithms but this relatively simple one already gives rather good results. Table 2 gives the results of the analysis for the sample of 200 events. The rows are the "true" identities of the tracks and the columns are the identities deduced using the above algorithm.

We see in Table 2 that 85% of all "real" kaons are called kaons by the RICH counters. On the other hand, of all tracks that are called kaons by the RICH counters, 88% of these are real kaons. As commented above, we are fairly confident that these efficiencies can be improved, as we use increasingly more sophisticated reconstruction algorithms.

Table 2: *RICH Counter Identification Matrix for 200 B_s Events***

		Identification from RICH counters			
		p	K	π	pKπ
"True" ID	p	22	22		26
	K	3	372	5	62
	π	10	30	1277	673

(*) For simplification, muons are not included here. Their contribution is small, however.